GEOPHYSICS, VOL. 63, NO. 1 (JANUARY-FEBRUARY 1998); P. 132–138, 7 FIGS., 1 TABLE.

Acoustic signatures of partial saturation

Rosemary Knight*, Jack Dvorkin‡, and Amos Nur‡

ABSTRACT

The relationship between elastic wave velocities and water saturation in a water/gas reservoir depends strongly on whether saturation is heterogeneous (patchy) or homogeneous. Heterogeneity in saturation may result from lithologic heterogeneity because under conditions of capillary equilibrium, different lithologies within a reservoir can have different saturations, depending on their porosities and permeabilities. We investigate this phenomenon by generating models of a reservoir in which we control the distribution of lithologic units and theoretically determine the corresponding velocity-saturation relationship. We assume a state of capillary equilibrium in the reservoir and determine the saturation level of each region within the reservoir from the corresponding capillary pressure curve for the lithologic unit at that location. The velocities we calculate for these models show that saturation heterogeneity, caused by lithologic variation, can lead to a distinct dependence of velocity on saturation. In a water-gas saturated reservoir, a patchy distribution of the different lithologic units is found to cause *P*-wave velocity to exhibit a noticeable and almost continuous velocity variation across the entire saturation range. This is in distinct contrast to the response of a homogeneous reservoir where there is only a large change in velocity at water saturations close to 100%.

INTRODUCTION

Elastic wave velocities in a partially saturated rock can be affected strongly by the saturation history and resulting fluid distribution. Over the past few years, there have been a number of laboratory and theoretical studies addressing the importance of fluid distribution in determining ultrasonic elastic wave velocities in rock samples (Endres and Knight, 1989; Knight and Nolen-Hoeksema, 1990; Endres and Knight, 1991; Cadoret, 1993; Mavko and Nolen-Hoeksema, 1994). Specifically, it has been found that the velocity is determined by the compliance and saturation state of the various regions of the pore space. In this way the saturation distribution at the pore scale and sample scale determines the observed velocity-saturation relationship for the rock sample.

Figure 1 shows laboratory data from Cadoret (1993) collected on a carbonate sample at frequencies of 1 and 100 kHz. This figure shows the variation in *P*-wave velocity V_P when the saturation is changed by imbibition and by drainage; in this case, saturation is the volume fraction of the pore space filled with water, with the remainder being filled with air. The imbibition process involved increasing saturation through the spontaneous uptake of water followed by depressurization of a saturated sample; the drainage process involved decreasing saturation through evaporative drying. During imbibition the velocity is almost constant or gently decreases with increasing saturation throughout most of the saturation range. Only at saturations very close to 1.0 does velocity show a very steep increase. The situation is quite different during drainage: velocity steadily decreases with decreasing saturation, passes a minimum, and then starts to gently increase. The same form of velocity-saturation behavior was observed in sandstones by Knight and Nolen-Hoeksema (1990) during an imbibition/drainage experiment. The differences between the imbibition and drainage ultrasonic data can be attributed to both pore-scale and sample-scale fluid distribution effects.

Theoretical modeling of pore-scale phenomena (Endres and Knight, 1991) and X-ray tomographic imaging of samples (Cadoret, 1993) have provided possible explanations for the differences observed between imbibition and drainage data. Our current understanding is that the imbibition process tends to create a homogeneous distribution of the two fluid phases, such that all pores, or regions of the pore space, contain both water and gas, resulting in a saturation that is approximately constant at all locations. In contrast, the drainage process creates a more heterogeneous saturation distribution at the pore scale and sample scale, with fully saturated pores or regions

Manuscript received by the Editor August 16, 1995; revised manuscript received October 31, 1996.
*Formerly Dept. of Geophysics, University of British Columbia; presently Dept. of Earth and Ocean Sciences, University of British Columbia, 2219 Main Mall, Vancouver, B.C. V6T 1Z4, Canada. E-mail: knight@geop.ubc.ca.
‡Dept. of Geophysics, Stanford University, Stanford, CA 94305-2215. E-mail: jack@pangea.stanford.edu.; nur@pangea.stanford.edu.

adjacent to partially saturated elements. The key difference between these two scenarios is the saturation state of the compliant or crack-like regions of the pore space: Full saturation with water can act to stiffen these compliant regions, thus increasing acoustic velocity.

The effective stiffening of compliant regions is a frequency-dependent phenomenon. At low frequencies, wave-induced pressure changes in the pore fluid quickly dissipate so that the pore-fluid pressure is very close to that of the high-compressibility gas in the dry pore space. As a result, the pore fluid accumulated in thin compliant pores can flow freely into the dry pore space (the squirt-flow effect) and does not act to reinforce the compliant part of the rock. However, at high frequencies this pressure equilibration does not take place because the pore-fluid relaxation time is greater than the wave's period. Pore fluid located in the thin compliant pores is therefore trapped, and its wave-induced pressure variations are relatively large. In this case, the fluid reinforces the compliant pores and thus acts to increase the apparent stiffness of the rock. The result is an increase in acoustic velocity.

This pore-scale process can repeat itself on a larger, macroscopic-patch scale. At low frequencies, pore fluid can flow easily between a saturated patch and the neighboring undersaturated rock. Thus the saturated patch behaves as a drained region in response to the passing wave. At sufficiently higher frequencies, pore fluid is trapped in the patch and the apparent stiffness of the patch becomes that of a fully saturated infinite rock region. The difference between the macroscopic squirt-flow effect and the pore-scale squirt-flow effect is that the pore-fluid relaxation time increases as the size of the volume occupied by the pore fluid increases. The size of a patch may be orders of magnitude larger than the size of a compliant pore. Therefore, if pore fluid is arranged in patches, the apparent stiffening of partially saturated rock in response to a sound wave may take place even at low frequencies.

Let us now consider the observed difference between the imbibition and drainage data. At low frequencies the bulk modulus of a saturated or partially saturated rock is related to that of a dry (or gas-saturated) rock through Gassmann's (1951) formula:

$$K_{\text{Saturated rock}} = K_{\text{Grain}} \times \frac{\phi K_{\text{Dry rock}} - \dfrac{(1+\phi)K_{\text{Fluid}}K_{\text{Dry rock}}}{K_{\text{Grain}}} + K_{\text{Fluid}}}{(1-\phi)K_{\text{Fluid}} + \phi K_{\text{Grain}} - \dfrac{K_{\text{Fluid}}K_{\text{Dry rock}}}{K_{\text{Grain}}}} \quad (1)$$

where ϕ is porosity, and K is the bulk modulus of the component indicated by the subscript. The shear modulus $G_{\text{Saturated rock}}$ of a saturated or partially saturated rock equals that of a dry rock. The bulk modulus of the pore fluid that is a liquid-gas mixture is related to the moduli of the components as

$$\frac{1}{K_{\text{Fluid}}} = \frac{S}{K_{\text{Liquid}}} + \frac{1-S}{K_{\text{Gas}}}, \quad (2)$$

where S is the level of liquid saturation. This description of the modulus of the pore fluid is valid for the low-frequency case, where fluid pressures equilibrate throughout the pore space. It is also valid at higher frequencies when there is a homogeneous fluid distribution, such as is presumed to exist during imbibition.

Let us assume certain reasonable values for the bulk moduli (K), density (ρ), porosity, and saturation:

$$K_{\text{Grain}} = 36.6\,\text{GPa}; \qquad K_{\text{Liquid}} = 2.25\,\text{GPa};$$

$$K_{\text{Gas}} = 0.04\,\text{GPa}; \qquad K_{\text{Dry rock}} = 15\,\text{GPa};$$

$$G_{\text{Dry rock}} = 17\,\text{GPa}; \qquad \phi = 0.2;$$

$$S = 0.8; \qquad \rho_{\text{Grain}} = 2650\text{kg/m}^3;$$

$$\rho_{\text{Liquid}} = 1000\,\text{kg/m}^3; \qquad \rho_{\text{Gas}} \ll \rho_{\text{Liquid}}.$$

If we consider a case where $S = 0.8$, formula (2) yields $K_{\text{Fluid}} = 0.187$ GPa. By substituting this value into formula (1) we

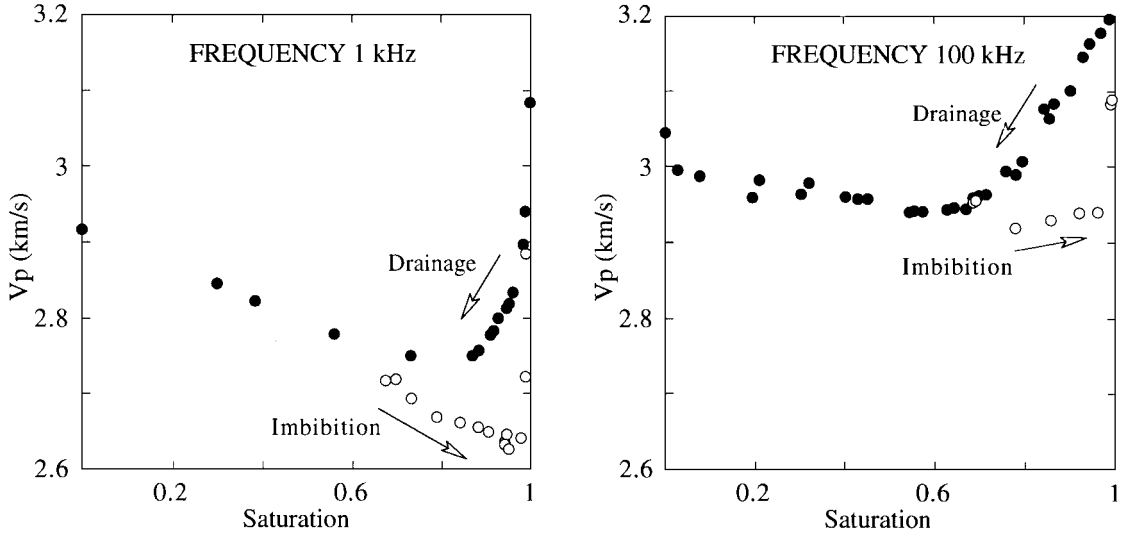

FIG. 1. Compressional-wave velocity versus saturation in a carbonate sample of about 30% porosity at 1 kHz and 100 kHz frequency (Cadoret, 1993). Open circles indicate imbibition; solid circles show drainage.

arrive at $K_{\text{Saturated rock}} = 15.32$ GPa. The corresponding compressional-wave velocity V_P can be obtained as

$$V_P = \sqrt{\left(K_{\text{Saturated rock}} + \tfrac{4}{3}G_{\text{Saturated rock}}\right)/\rho},$$
$$\rho = (1-\phi)\rho_{\text{Grain}} + \phi S\rho_{\text{Liquid}} + \phi(1-S)\rho_{\text{Gas}}. \quad (3)$$

Formula (3) yields $V_P = 4082$ m/s. This value is only 0.4% larger than the dry-rock velocity of 4065 m/s. Therefore if liquid and gas are mixed at the pore scale, the velocity shows a negligible increase even at a high level of liquid saturation.

Let us now consider a second case, again with $S = 0.8$, but assume that all the liquid is concentrated in fully saturated regions that neighbor completely dry regions. Let us also assume that the frequency is high enough so that a saturated region has the stiffness of the fully saturated rock. Formula (1) yields the bulk modulus of the fully saturated rock as $K_{\text{Saturated rock}} = 18.5$ GPa. The corresponding velocity is $V_P = 4249$ m/s, a 4% increase from the velocity of the dry rock. Now we have partially saturated rock that is a composite of two phases—fully saturated rock and dry rock. The volumetric concentration of the fully saturated regions is $f_{\text{Saturated}} = 0.8$, whereas that of dry regions is $f_{\text{Dry}} = 0.2$. The shear moduli of these two phases are identical. For such a situation, Hill (1963) provides the following formula for the effective V_P in the composite:

$$\frac{1}{\rho V_P^2} = \frac{f_{\text{Saturated}}}{\rho_{\text{Sat}} V_{P\,\text{Sat}}^2} + \frac{f_{\text{Dry}}}{\rho_{\text{Dry}} V_{P\,\text{Dry}}^2}, \quad (4)$$

where ρ_{Sat} and $V_{P\,\text{Sat}}$, and ρ_{Dry} and $V_{P\,\text{Dry}}$ are the densities and velocities of the fully saturated rock, and of the dry rock, respectively. By using formula (4), we obtain $V_P = 4209$ m/s. This value is much higher than the velocity of 4082 m/s predicted for the rock where liquid and gas are mixed at the pore scale and can explain the difference between the drainage and the imbibition data points in Figure 1. The heterogeneous saturation distribution during drainage results in an effective stiffening of water-saturated pores and patches. This causes a higher velocity than is seen during imbibition when the water and gas are homogeneously distributed throughout the pore space.

The purpose of our present study is to apply this same concept on a larger scale to investigate the dependence of velocity on saturation in a water/gas reservoir. If a reservoir is composed of regions of varying rock types, at any given reservoir-scale saturation the regions of the reservoir can have different local saturation levels. Saturation heterogeneity can exist at the reservoir scale such that there are fully water-saturated regions adjacent to partially saturated regions. The velocity-saturation relationship at the reservoir scale will then be determined by the velocity and saturation state of the various regions of the reservoir. The key is to incorporate the control on the heterogeneity of local saturation in our models of a reservoir.

In this study we link saturation heterogeneity to the lithologic heterogeneity in a reservoir by assuming a state of capillary equilibrium. Then regions, or patches, in the reservoir of different lithologies will have different levels of saturation, as determined from their capillary pressure curves. The velocity dependence on saturation in each homogeneous region can be described with Gassmann's equation. At the reservoir scale, however, the variation in velocity with saturation is much more complicated because of saturation heterogeneity. We find that velocities can be sensitive to gas saturation, with the specific form of dependence on saturation level determined by the volume fraction and distribution of rock types.

It is important to emphasize that capillary pressure curves are affected strongly by permeability. Therefore, a critical factor that controls saturation heterogeneity and thus velocity in a partially saturated reservoir is the permeability of the different lithologies. This effect opens a potential avenue for inferring the permeability distribution from velocity data.

QUANTITATIVE MODEL

Saturation

In each reservoir model, we assume a state of capillary equilibrium such that capillary pressure everywhere is constant; gravitational forces are neglected. The level of water saturation S in a homogeneous region is related to capillary pressure using the relationship determined by Brooks and Corey (1964):

$$S = S_{irr} + (1 - S_{irr})\left(\frac{P_t}{P_c}\right)^{\lambda}, \quad (5)$$

where S_{irr} is the irreducible water saturation, P_t is the threshold pressure, P_c is the capillary pressure, and λ is constant for a given lithology. The threshold pressure is a property of the rock type and is a measure of the gas pressure required to initiate the displacement of water. We use the relation between P_t and permeability k given in Thomas et al. (1968) as

$$P_t = 52k^{-0.43}, \quad (6)$$

where pressure is in kilopascals (kPa) and permeability is in microdarcies (mD). Irreducible water saturation is linked to permeability in Timur's (1968) empirical equation

$$S_{irr} = 11.59\frac{\phi^{1.26}}{k^{0.35}} - 0.01, \quad (7)$$

where permeability is in mD. Both saturation and porosity in this equation are given as a fraction of one, not as a percentage.

Equations (5)–(7) are empirical relations and thus lack generality, but provide a means of quantifying the saturation heterogeneity likely to occur in a reservoir. Figure 2 shows schematic capillary pressure curves for two rocks with contrasting permeabilities. Under the conditions of capillary equilibrium, where P_c is the same for the two rocks, it is apparent that two neighboring lithologies can have very different fluid saturations. In the example shown in Figure 2, at the selected capillary pressure, the low-permeability rock is fully water-saturated while the high-permeability rock is at a saturation of about 0.35.

If a reservoir is composed of n different rock types, or lithologic units, with the volume fraction of the ith rock type f_i, then the effective (global) saturation of the reservoir S_g can be related to the local saturations S_i and porosities ϕ_i as

$$S_g = \frac{\sum_{i=1}^{n} S_i \phi_i f_i}{\sum_{i=1}^{n} \phi_i f_i}. \quad (8)$$

By using equations (5)–(8), and knowing the volume fractions of different rock types in the reservoir and their permeabilities and porosities, we can relate global saturation to capillary pressure.

Velocity

In our calculation of velocities, we assume that the reservoir can be divided into a number of small regions or patches where each patch is isotropic and composed of a single rock type. We assume that the reservoir itself can be treated as an isotropic effective medium with n constituents. If the elastic moduli of each rock type are known, then an effective medium theory can be applied to calculate the reservoir's effective elastic moduli. In this study, we use a static effective medium theory, Hashin-Shtrikman bounds, and therefore an important limitation is that the size of each patch is significantly smaller than a wavelength.

We assume that the bulk modulus of each of the lithologic patches can be estimated from Gassmann's formula (1) with the bulk modulus of the pore fluid given by equation (2). This use of Gassmann's formula implies that a fully saturated patch that neighbors an undersaturated region is large enough that at seismic frequencies the patch has the stiffness of the fully saturated infinitely large rock region; that is, it behaves as an undrained system. A criterion for the size of a patch is given below.

The Hashin-Shtrikman bounds for the effective bulk modulus K_{eff} are (Berryman, 1995):

$$\left[\sum_{i=1}^{n}\frac{f_i}{K_i+\frac{4}{3}G_{\min}}\right]^{-1}-\frac{4}{3}G_{\min}\le K_{\text{eff}} \le\left[\sum_{i=1}^{n}\frac{f_i}{K_i+\frac{4}{3}G_{\max}}\right]^{-1}-\frac{4}{3}G_{\max}, \tag{9}$$

where K_i is the bulk modulus of the ith lithologic unit, and $G_{\min}$ and $G_{\max}$ are the minimum and the maximum shear modulus among the n lithologic units, respectively. The bounds for the effective shear modulus G_{eff} are

$$\left[\sum_{i=1}^{n}\frac{f_i}{G_i+\frac{G_{\min}}{6}\left(\frac{9K_{\min}+8G_{\min}}{K_{\min}+2G_{\min}}\right)}\right]^{-1}-\frac{G_{\min}}{6}\left(\frac{9K_{\min}+8G_{\min}}{K_{\min}+2G_{\min}}\right)\le G_{\text{eff}} \le\left[\sum_{i=1}^{n}\frac{f_i}{G_i+\frac{G_{\max}}{6}\left(\frac{9K_{\max}+8G_{\max}}{K_{\max}+2G_{\max}}\right)}\right]^{-1}-\frac{G_{\max}}{6}\left(\frac{9K_{\max}+8G_{\max}}{K_{\max}+2G_{\max}}\right), \tag{10}$$

where G_i is the shear modulus of the ith lithologic unit, and $K_{\min}$ and $K_{\max}$ are the minimum and the maximum bulk modulus among the n lithologic units, respectively.

The effective P- and S-wave velocities ($V_{P\,\text{eff}}$ and $V_{S\,\text{eff}}$, respectively) are calculated as

$$V_{P\,\text{eff}}=\sqrt{\left(K_{\text{eff}}+\tfrac{4}{3}G_{\text{eff}}\right)/\rho_{\text{eff}}},\qquad V_{S\,\text{eff}}=\sqrt{G_{\text{eff}}/\rho_{\text{eff}}}, \tag{11}$$

where ρ_{eff} is the effective (average) density of the reservoir.

By using equations (1), (2), and (5)–(11), we can calculate the upper and the lower bounds for the effective P- and S-wave velocities in a reservoir versus global saturation.

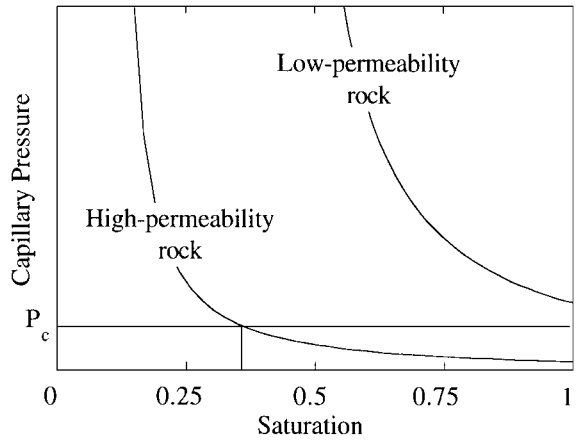

FIG. 2. Schematic capillary pressure curves for a low-permeability and a high-permeability rock. At the same capillary pressure P_c these two neighboring lithologies may have different saturations. The low-permeability rock is fully saturated, whereas the high-permeability rock has a saturation of about 0.35.

Limits for patch size

The final aspect of our model that must be considered is the length-scale associated with the saturation heterogeneity. Based on the squirt-flow model presented in Dvorkin et al. (1993), we use the following criterion for the minimum characteristic size D of a finite-size patch at which the patch has the stiffness of the equally saturated infinitely large rock region:

$$\frac{fD^2}{\kappa}>10, \tag{12}$$

where f is frequency and κ is the diffusivity of rock. The diffusivity is given as

$$\kappa=\frac{kF}{\mu\phi},\qquad \frac{1}{F}=\frac{1}{K_{\text{Fluid}}}+\frac{1-\phi-K_{\text{Dry rock}}/K_{\text{Grain}}}{\phi K_{\text{Grain}}},$$

where k is rock permeability and μ is fluid viscosity.

Equation (12) provides the lower limit for the size of a patch as acceptable in our formulation. As mentioned above, this size has to be much smaller (at least 10 times) than the wavelength l. Finally, we arrive at the following bounds for D:

$$\sqrt{\frac{10\kappa}{f}}<D<\frac{l}{10}. \tag{13}$$

Consider, for example, a water-filled Fontainbleau sandstone sample of porosity 0.136 and permeability 670 mD (Lucet, 1989). In this case,

$$\phi = 0.136, k = 0.67 \cdot 10^{-12}\ \mathrm{m}^2, \mu = 10^{-3}\ \mathrm{Pa} \cdot s,$$

$$K_{\mathrm{Dry\ rock}} = 23.7 \cdot 10^9\ \mathrm{Pa},$$

$$K_{\mathrm{Grain}} = 36.6 \cdot 10^9\ \mathrm{Pa}, K_{\mathrm{Fluid}} = 2.25 \cdot 10^9\ \mathrm{Pa}.$$

Then, for example, at 50-Hz frequency, the lower limit for D is about 1.5 m. It is clear from formula (13) that for a rock with smaller permeability, this bound will be even smaller. If the P-wave velocity is 4.5 km/s then the wavelength is 90 m and formula (13) yields 1.5 m $< D <$ 9 m.

EXAMPLES

Two lithologic units

For our first example, we assume that a reservoir is composed of two lithologies: clean sand and shaley sand (about 10% volumetric clay content). The necessary data for these two components are taken from Yin (1993) and summarized in Table 1. It is assumed that the rock is at 30 MPa effective pressure. Parameter λ in equation (5) is selected to be 0.9.

P-wave velocity versus water saturation in the two pure lithologies (clean sand and shaley sand) are calculated using Gassmann's formula and given in Figure 3. The effect of saturation is well pronounced only in the immediate vicinity of full saturation. For example, in the shaley sand the difference between the velocities at 80% saturation and 90% saturation is nonexistent, whereas the difference between the velocities at 95% saturation and 100% saturation is about 240 m/s.

We now consider three reservoir models where these two lithologies are arranged as patchy mixtures with the total volume fraction of the clean sand equal to 0.7, 0.5, and 0.2. P-wave velocity versus *global* saturation for these three mixtures is shown in Figure 4. In this case, noticeable velocity changes occur not only in the vicinity of full saturation but also at lower saturations. The reason is that at global saturations below 100%, the clean sand can be partially saturated, while the shaley sand remains fully saturated. Therefore the transition from the undersaturated, low-velocity behavior to the fully saturated, high-velocity behavior occurs in the shaley sand at global saturations below 100%. These transitions can be seen in Figure 4 as the "kinks" in the velocity-saturation curves at intermediate saturations.

In our next reservoir model, we set the volume fraction of the clean sand equal to 0.4 and consider two mixtures of the clean sand and the shaley sand. In the first mixture the lithologies are arranged in a patchy way, whereas in the second mixture the lithologies are homogeneously mixed at the grain-scale level. This second mixture is equivalent to a shaley sand with about 6% volumetric clay content; the necessary data for this mixture are given in Table 1. The calculated velocities versus saturation for both mixtures are given in Figure 5. It is evident that the velocity-saturation function can be affected strongly by the way the two lithologies are mixed: in a patchy arrangement, strong velocity variations occur at intermediate saturations whereas in the homogeneous mixture case, these variations are concentrated at 100% saturation.

Table 1. Permeability, porosity, elastic moduli, and density for sand-clay mixtures at 30 MPa effective pressure.

	Sand	Shaley sand (10% clay)	Shaley sand (6% clay)
ϕ (fraction)	0.34	0.27	0.32
k (mD)	2000	20	200
$K_{\mathrm{Dry\ rock}}$ (GPa)	9.2	12	11
$G_{\mathrm{Dry\ rock}}$ (GPa)	2.2	1.7	1.7
K_{Grain} (GPa)	36.6	34.5	35.3
ρ_{Grain} (g/cm^3)	2.65	2.643	2.645

Multiple lithologic units

Our final two reservoir models are composed of 10 different lithologies. Each lithology is a sand-clay mixture with the volumetric clay content varying from zero to 22.5%. We assume that the effective pressure is 10 MPa and take the values of porosity, permeability, and dry-rock bulk and shear moduli from Yin (1993). These values are plotted in Figure 6 as clay content and permeability versus porosity (a), and elastic moduli versus porosity (b). As before, parameter λ in equation (5) is selected to be 0.9.

We first arrange the 10 lithologies as a patchy mixture and apply the above quantitative model to calculate V_P versus saturation in the "patchy" reservoir. In this reservoir model, the patchy nature of the lithologic distribution leads to considerable spatial heterogeneity in saturation level. The resulting velocity-saturation relationship, shown in Figure 7a, is a noticeable and almost continuous velocity variation in the saturation range between 60 and 100%.

In our final reservoir model we assume that the volumetric distribution of the 10 lithologic units is uniform; thus the volumetric fraction of each unit is 0.1. If we assume that the mixture under consideration is not patchy, but that sand and clay are mixed at the grain scale, we arrive at the effective volumetric clay content of 11.25%. The corresponding velocity-saturation

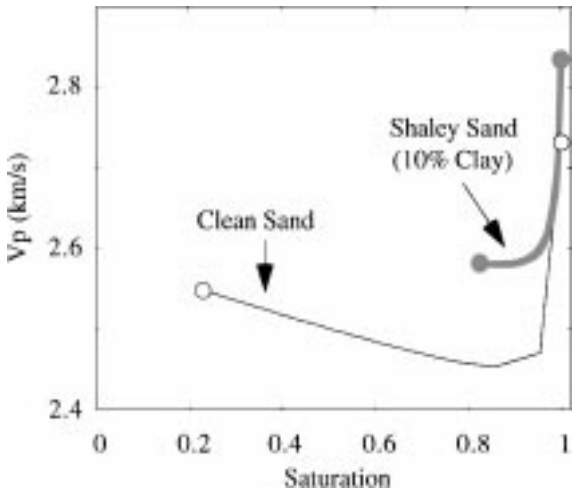

FIG. 3. P-wave velocity versus saturation for clean sand and for shaley sand. The open and solid circles indicate the end values of the velocity for the clean sand and shaley sand, respectively. Each curve starts at the irreducible water saturation; that is, 0.2 for the clean sand and 0.8 for the shaley sand.

function in this homogeneous mixture is shown in Figure 7b. In this case a strong velocity variation occurs only in the vicinity of full saturation.

CONCLUSIONS

Under conditions of capillary equilibrium, different lithologies within a reservoir can have different saturations, depending on their porosities and permeabilities. We have shown that such reservoir-scale heterogeneity in saturation (caused by heterogeneity in lithology) has a significant effect on the form of the velocity-saturation relationship. A patchy distribution of different lithologic units may cause *P*-wave velocity to exhibit a noticeable and almost continuous velocity variation across the entire saturation range. Such a situation is markedly different from one in which the water and gas are homogeneously distributed at the pore scale and reservoir scale. In this case, a velocity variation is large only at water saturations close to 100% and can be used only to distinguish between the presence of no gas (fully water-saturated) and some gas (partially water-saturated).

The presented model, that uses lithologic information as input, serves to illustrate the effect that saturation heterogeneity could have on field seismic data. This model assumes a priori knowledge of the types and distribution of lithologies, thus cannot be directly applied to the interpretation of seismic data. In this study we have developed a theoretical basis for quantifying the link between the spatial variation that exists in lithology and the corresponding acoustic signature of partial saturation.

ACKNOWLEDGMENTS

This work was supported by funding to Rosemary Knight from Conoco and Petro-Canada, and to Jack Dvorkin and Amos Nur from the Gas Research Institute, contract 5094-210-34125.

REFERENCES

Berryman, J. G., 1995, Mixture theories for rock properties, *in* Ahrens, T. J., Ed., Rock physics and phase relations: AGU Reference Shelf 3.

Brooks, R. H., and Corey, A. T., 1964, Hydraulic properties of porous media: Hydrology Paper No. 3, Colorado State University.

Cadoret, T., 1993, Effect de la saturation eau/gaz sur les proprieties acoustics des roches: Ph.D. thesis, University of Paris VII.

Dvorkin, J., Nolen-Hoeksema, R., and Nur, A., 1993, The squirt-flow mechanism: Macroscopic description: Geophysics, **59**, 428–438.

Endres, A. L., and Knight, R., 1989, The effect of microscopic fluid distribution on elastic wave velocities: Log Analyst, **30**, 437–445.

———1991, The effects of pore scale distribution of fluids on the physical properties of partially saturated tight sandstones: J. Appl. Phys., **69**, 1091–1098.

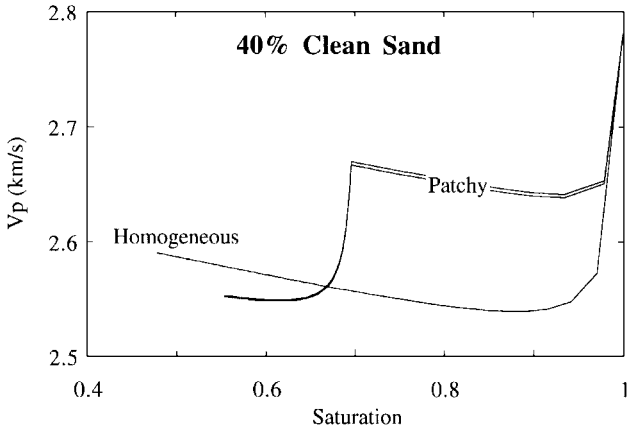

FIG. 5. *P*-wave velocity versus saturation in a mixture of the clean sand and the shaley sand with 40% volumetric fraction of clean sand. The two lithologies are combined in a patchy arrangement and as a homogeneous mixture. In the results for the patchy arrangement the upper and lower bounds are very close and appear as a single curve.

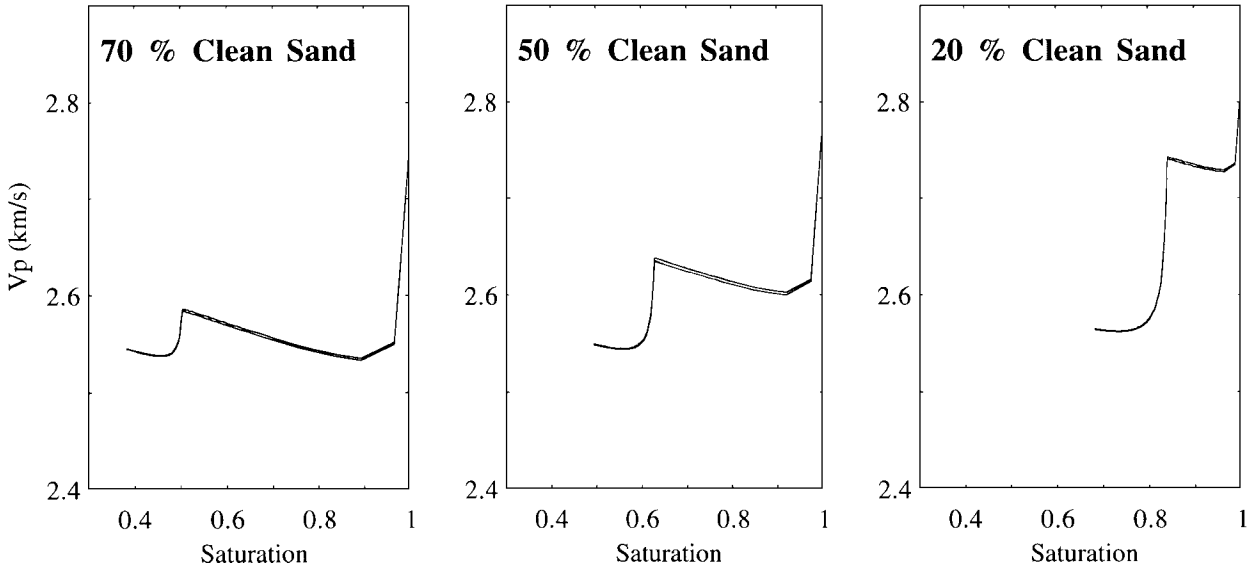

FIG. 4. *P*-wave velocity versus saturation for mixtures of the clean sand and the shaley sand. Both upper and lower bounds are calculated using formulas (9) and (10). These bounds are very close and appear as a single curve.

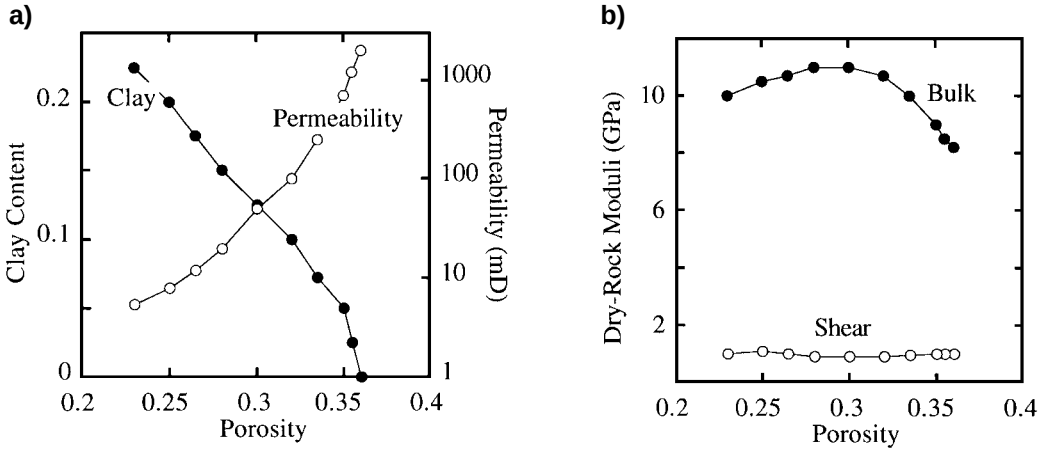

FIG. 6. Properties of the 10 lithological units. (a) Clay content and permeability versus porosity. (b) Dry-rock bulk and shear moduli versus porosity.

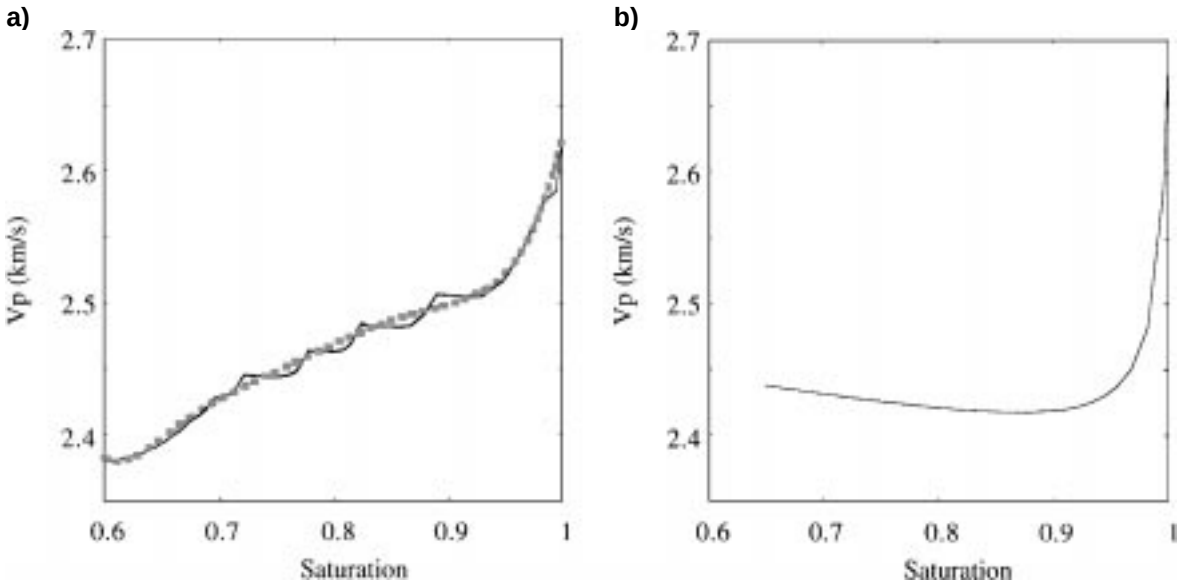

FIG. 7. (a) Velocity versus saturation in a patchy mixture of ten lithological units. The dotted curve is a polynomial fit. (b) Velocity versus saturation in a pore-scale mixture of ten lithological units.

Gassmann, F., 1951, Uber die elastizitat poroser medien: Veir der Natur Gesellscheft, **96**, 1091–1098.
Hill, R., 1963, Elastic properties of reinforced solids: Some theoretical principles: J. Mech. Phys. Solids, **11**, 357–372.
Knight, R. J., and Nolen-Hoeksema, R., 1990, A laboratory study of the dependence of elastic wave velocities on pore scale fluid distribution: Geophys. Res. Lett., **17**, 1529–1532.
Lucet, N., 1989, Vitesse ey attenuation des ondes elastiques soniques et ultrasoniques dans les roches sous pression de confinement: Ph.D. thesis, University of Paris.
Mavko, G., and Nolen-Hoeksema, R., 1994, Estimating seismic velocities at ultrasonic frequencies in partially saturated rocks: Geophysics, **59**, 252–258.
Thomas, L. K., Katz, D. L., and Tek, M. R., 1968, Threshold pressure phenomena in porous media: Soc. Petrol. Eng. J., **243**, 174–184.
Timur, A., 1968, An investigation of permeability, porosity, and residual water saturation relationships for sandstone reservoirs: The Log Analyst, 8–17.
Yin, H., 1993, Acoustic velocity and attenuation of rocks: Isotropy, intrinsic anisotropy, and stress-induced anisotropy, Ph.D. thesis, Stanford University.